Science of the Total Environment 848 (2022) 157779

Contents lists available at ScienceDirect

Science of the Total Environment

journal homepage: www.elsevier.com/locate/scitotenv

Copper (Cu) speciation in organic-waste (OW) amended soil: Instability of OW-borne Cu(I) sulfide and role of clay and iron oxide minerals

Thiago A. Formentini [a,f,*], Isabelle Basile-Doelsch [b], Samuel Legros [c,i], Andrew J. Frierdich [d], Adilson Pinheiro [e], Cristovão V.S. Fernandes [f], Fábio J.K. Mallmann [g], Daniel Borschneck [b], Milton da Veiga [h], Emmanuel Doelsch [c,i]

[a] Department of Soil and Environment, Swedish University of Agricultural Sciences, P. O. Box 7014, SE-750 07 Uppsala, Sweden
[b] Aix-Marseille Université, CNRS, IRD, Coll France, INRA, CEREGE, F-13545 Aix-en-Provence, France
[c] CIRAD, UPR Recyclage et risque, F-34398 Montpellier, France
[d] School of Earth, Atmosphere & Environment, Monash University, Clayton, Victoria, Australia
[e] Environmental Engineering Program, Regional University of Blumenau (FURB), 89030-000 Blumenau, SC, Brazil
[f] Department of Hydraulics and Sanitation, Federal University of Parana (UFPR), 81531-980 Curitiba, PR, Brazil
[g] Department of Soils, Federal University of Santa Maria (UFSM), 97105-900 Santa Maria, RS, Brazil
[h] UNOESC, P.O. Box 250, 89620-000 Campos Novos, SC, Brazil
[i] Recyclage et Risque, Univ. Montpellier, CIRAD, Montpellier, France

HIGHLIGHTS

- Long-term field study with 22 applications of pig slurry over 11 years.
- Cu in the pig slurry was 100 % Cu (I) sulfide, which did not persist in the soil.
- Pig-slurry borne Cu was retained by soil constituents, mostly kaolinite.
- Cu dimer observed in the interlayer of vermiculite in natural soil.
- Cu structurally incorporated within hematite in natural soil.

GRAPHICAL ABSTRACT

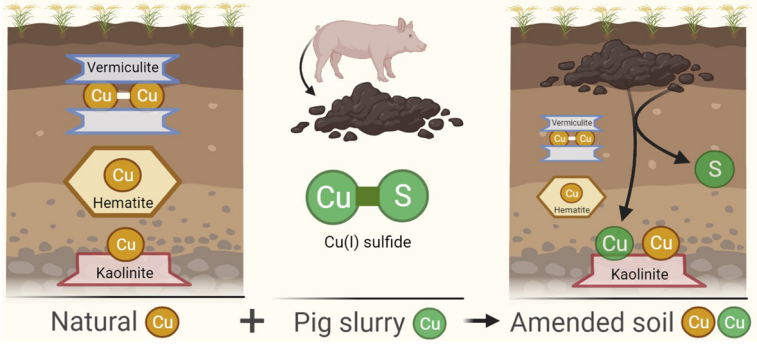

ARTICLE INFO

Editor: Mae Sexauer Gustin

Keywords:
XAS
Cu dimer
Cu-vermiculite
Cu-hematite
Cu-kaolinite
Pig slurry
Agricultural recycling

ABSTRACT

The geochemistry of copper (Cu) is generally assumed to be controlled by organic matter in soils. However, the role of clay and iron oxide minerals may be understated. Soil density fractionation, X-ray diffraction (XRD), and X-ray absorption spectroscopy (XAS) were combined to assess the long-term behavior of Cu in an agricultural soil subject to organic waste application. Two unprecedented molecular environments of natural Cu (i.e. Cu inherited from the parent rock) in soils are reported: Cu dimer in the interlayer of vermiculite and Cu structurally incorporated within hematite. Moreover, the soil naturally containing Cu-vermiculite, Cu-hematite, but also Cu-kaolinite (Cu_{total} = 122 mg·kg^{-1}) was amended over 11 years with Cu-rich pig slurry in which Cu was 100 % Cu(I) sulfide. Natural Cu associated with clay and iron oxide minerals persisted in the amended soil, but the exogenous Cu(I) sulfide was unstable. The increase in Cu concentration in the amended soil to 174 mg·kg^{-1} was accounted for the increase of Cu sorbed to kaolinite and Cu bound to organic matter. These results are important for better understanding the natural occurrence of Cu in soils and for assessing the environmental impacts of organic waste recycling in agricultural fields.

* Corresponding author at: Department of Soil and Environment, Swedish University of Agricultural Sciences, P. O. Box 7014, SE-750 07 Uppsala, Sweden.
E-mail address: thiago.formentini@slu.se (T.A. Formentini).

http://dx.doi.org/10.1016/j.scitotenv.2022.157779
Received 11 April 2022; Received in revised form 28 July 2022; Accepted 29 July 2022
Available online 1 August 2022

1. Introduction

Copper (Cu) compounds are supplemented in the diets of pigs to control diseases and promote growth (Edmonds et al., 1985). High Cu concentrations in livestock feeds ensure that sufficient levels will be taken up by the animals. European regulation 2018/1039 of 23 July 2018 limits Cu in pig feeds at a maximum 150 $mg.kg^{-1}$ up to four weeks after weaning and 100 $mg.kg^{-1}$ from five to eight weeks after weaning. Still, most Cu is excreted rather than absorbed and ultimately applied to agricultural land as Cu-rich livestock manure. Increased Cu levels in soils may lead to phytotoxicity (Yang et al., 2002), introduction in the food chain (Vincevica-Gaile and Klavins, 2012), and groundwater contamination (Paradelo et al., 2013). Studying the long-term behavior of Cu in manure-amended soil is important to evaluate the risk associated with Cu addition in livestock feed.

It is widely accepted that the biogeochemistry of Cu is controlled by its interactions with natural organic matter (OM) (Manceau and Matynia, 2010), and that the OM fraction of the soil is of primary importance in binding Cu in the soils (Strawn and Baker, 2009). Nevertheless, clay and iron oxide minerals play an important role in the Cu geochemistry too. For instance, Ramos et al. (1994) and McBride and Bouldin (1984) found Cu mostly in the mineral residual fractions in nine out of 19 contaminated soils. McBride and Martínez (2000) showed that alumina and ferrihydrite were effective in binding Cu within a contaminated soil, which was not observed for soil OM. McBride et al. (1997) evaluated soluble Cu in soils as a function of total Cu, pH, and OM, concluding that solubility of Cu was not significantly correlated with OM content.

Synchrotron radiation, particularly X-ray absorption spectroscopy (XAS), can directly probe the molecular environment of Cu in soils. Flogeac et al. (2004) and Boudesocque et al. (2007) proposed that Cu was bound to OM coated onto the mineral fraction of soil particles. However, Cu was spiked as soluble salts and XAS analysis was limited to the first coordination shell (Cu—O geometry and bond distances). Strawn and Baker (2009) investigated contaminated soils using XAS and reported Cu–OM complexes in the form of five membered ring chelates.

Yamamoto et al. (2018) reported 95 % of Cu associated with minerals in a non-contaminated soil using XAS. After 23 years applying swine manure compost containing mostly Cu bound to organic matter, Cu–OM accumulated in the soil together with the natural Cu species. The minerals associated with Cu in the non-contaminated soil could not be unambiguously asserted, because the XAS fingerprint for Cu sorbed to phyllosilicates and to oxides was similar. A biosolid-amended calcareous loamy soil containing clays and OM showed only 41 % Cu associated to OM, with the remaining fraction in the form of $Cu_2(CO_3)(OH)_2$, as assessed via XAS (Mamindy-Pajany et al., 2014).

The above examples illustrate that the geochemistry of Cu in natural and contaminated soils is exceptionally complex. Probable reasons for the Cu–OM oversimplification include: (i) laboratory experiments provide insights for well-delimited systems, but may fail to reproduce the complexity found in the field; (ii) the nature of low-proportion Cu species is usually ignored, because chemical extractions or XAS have low sensitivity for minor species; (iii) mixed species showing similar XAS signature are difficult to distinguish; and (iv) Cu speciation in the source of contamination (e.g. livestock waste or sewage sludge) is seldom taken into account. These scientific gaps and challenges represented the main motivation of the present study and were all taken into account.

The objective of this study was to assess the impact of long-term application of Cu-rich pig slurry to agricultural soil. The Cu speciation in pig slurry, in contaminated soil (i.e., amended with slurry for 11 years), and in non-contaminated soil (un-amended with slurry) were studied. A density fractionation procedure was applied to reduce the soil matrix complexity by isolating different soil phases that allowed for the identification and quantification of minor Cu species. X-ray diffraction (XRD) and XAS were combined to analyze the density fractions, the bulk soils, and the pig slurry. The speciation of Cu was assessed based on key XAS spectral features and by comparing the spectra with a comprehensive database of XAS model compounds using linear combination fitting (LCF).

2. Experimental section

2.1. Soils and pig slurry

The studied soil was a basaltic Rhodic Hapludox (USDA, 2003) containing 67.8 % clay, 30.8 % silt, and 1.4 % sand located in Campos Novos, SC, Brazil. The soil was developed from intermediate effusive rock saprolites of Serra Geral formation. The experiment consisted of 6-m long, 5-m wide agricultural plots positioned side by side in the field in three replicate blocks and maintained and monitored over 11 years at exact same conditions. One treatment (in triplicate) consisted of mineral fertilization using triple superphosphate (42 % P_2O_5) and potassium chloride (60 % K_2O) to replace P and K exported through harvests. This control soil is denoted PK-soil (P and K fertilization), and contained only natural Cu inherited from the parent rock. The other treatment (in triplicate) consisted of fertilizing the soil with 200 $m^3 \cdot ha^{-1} \cdot year^{-1}$ of pig slurry, an incidental source of Cu contamination. This soil is denoted OW-soil (organic waste fertilization).

Soil samples were collected in 2011, after 11 years of inorganic or pig slurry fertilization, air dried, crushed, sieved through a 2.0 mm mesh sieve and stored in plastic containers prior to analysis. Samples were stored at oxic conditions (as in the field) after air drying, which preserves trace metal speciation for several years (Davidson et al., 1999; Ure et al., 1995). Information on the Cu distribution along the soil profile, crop rotations, seeding, and sampling may be found elsewhere (Formentini et al., 2017; Formentini et al., 2015; Veiga et al., 2012). It was previously reported that most of the pig-slurry borne Cu applied onto the OW-soil (200 $m^3 \cdot ha^{-1} \cdot year^{-1}$) accumulated within the uppermost soil layer (0–5 cm) and that Cu standard deviations between replicate blocks were very low (Formentini et al., 2015). Therefore, the 0–5 cm layer of one PK-soil replicate and one OW-soil replicate, both collected from the same block, were used for exploring their Cu molecular environment in the present study. A fresh pig slurry sample was collected in the anaerobic lagoon that had provided the organic wastes applied to the OW-soil throughout the entire experiment duration, as it best represents the Cu speciation in the pig slurry at the moment it was spread. The anaerobic conditions in this sample were preserved by collecting it near the bottom of the lagoon, by storing it in a sealed container without air, and by keeping it in the dark at 4 °C for a few hours during transport prior to freeze drying (−53 °C). The interval between sampling and XAS analysis was one week only.

2.2. Density fractionation

Soil samples were subjected to density fractionation in triplicates in 2014, as previously reported elsewhere (Formentini et al., 2021) and described in details in Supporting Information SI-4. Briefly, sodium polytungstate solutions (LST) with different densities were used to isolate five soil density fractions: >2.7 $g \cdot cm^{-3}$ (denoted heavy fraction), 2.5–2.7 $g \cdot cm^{-3}$ (denoted intermediate fraction), 2.25–2.5 $g \cdot cm^{-3}$, 1.9–2.25 $g \cdot cm^{-3}$ (denoted other fractions), and < 1.9 $g \cdot cm^{-3}$ (denoted light fraction).

The mineralogy of the density fractions was qualitatively assessed using an X-ray diffractometer (X'Pert Pro, Panalytical) running at 40 kV and 40 mA, using Co Kα radiation (λ = 1.79 Å) with a linear detector (X'Celerator) and a secondary flat monochromator. Moreover, the clay fraction of the bulk PK-soil was isolated and treated with solvation in ethylene glycol, heating at 300 °C for 4 h, and heating at 490 °C for 4 h. The XRD diffractograms recorded after each of these treatments were used to confirm the presence of vermiculite and kaolinite in the soil (Section 3.1). The soil mineralogy assessed using XRD was used to guide the selection of reference compounds potentially associated with Cu in the quantitative LCF procedure (XAS, Section 2.3).

Total organic carbon (TOC) in bulk soils and density fractions was measured using an elemental analyzer (NA 1500, Fisons). For Cu analysis, bulk soils and density fractions were subjected to microwave-assisted acid digestion according to the EPA 3051A protocol (USEPA, 2007) and then diluted in 2 % HNO_3 (PlasmaPure Plus 69 % HNO_3, SCP Science; Milli-Q Reference

Ultrapure Water, Millipore). Concentrations were measured by inductively coupled plasma mass spectrometry (ICP-MS, NexION 300×, PerkinElmer) with online addition of Rh-103 as internal standard element. The ICP-MS measurement accuracy was checked using certified reference samples [SLRS-5 river water, Canada; GBW07402 (GSS-2) and GBW07403 (GSS-3) soils, China].

2.3. XAS analysis

The Cu K-edge XAS for the bulk PK-soil, bulk OW-soil, their respective density fractions, and the pig slurry were recorded in 2014 and 2015 on the FAME beamline (BM30B) at the ESRF, Grenoble, France. Dry samples were finely ground, pressed into pellets and analyzed at liquid He temperature to avoid Cu photoreduction. The signal was acquired in fluorescence mode using a 30 element solid-state Ge detector (CANBERRA Industries Inc.). Energy calibration was performed using metallic Cu reference foil (absorption edge defined at 8979 eV and taken at the zero crossing point of the second derivative spectrum). The spectra for the soils and density fractions were the sum of nine to 16 scans, depending on the Cu concentration and the noise level. The spectrum for the pig slurry was the sum of three scans.

Normalization and background removal were performed using the AUTOBK function in the Athena software (Ravel and Newville, 2005) setting rbkg = 1, k-weight = 3, and E_0 = 8987 eV for all samples. Fourier transforms (FT) were performed in the χ(k) region between 2.25 and 10 $Å^{-1}$ into χ(R) using a Kaiser-Bessel apodization window (dk = 1). Backward FT was performed using a Kaiser-Bessel window to isolate the contributions of the coordination shells in real space [χ(R)] and turn them back into k space [χ(k)]. Fourier transform peaks are uncorrected from phase shift functions, i.e. they are displaced from crystallographic distances by about 0.3–0.4 Å.

Background subtracted and normalized EXAFS spectra were subjected to least-square LCF over the k-range 3.5–10 $Å^{-1}$ on k^2-weighed spectra, as this region captured the key features in the samples and had a low noise level. LCF aimed to identify and quantify the Cu species in each sample using a library of Cu model compounds including (but not limited to) Cu associated with minerals identified via XRD, such as Cu bound to organic functional groups, Cu-containing minerals, and Cu sorbed/incorporated onto Fe (hydr)oxides and phyllosilicates. The Cu model compounds are presented in Supporting Information SI-2.

Initial LCF scenarios using one component were tracked regarding the improvement to the value of the residual factor R [$R = \Sigma(k^2\chi_{exp} - k^2\chi_{model})^2 / \Sigma(k^2\chi_{exp})^2$] and to key visual EXAFS features when passing from one- to two-component and from two- to three-component LCF scenarios. LCFs with $n + 1$ components were used as the optimal solution if the R factor was decreased by >20 % as compared to the fit with n components. The sum of component weights in the best LCFs ranged from 98 % to 119 %. LCF results were normalized to 100 % to compare the relative speciation between samples. The uncertainty for the LCF procedure is assumed around 15 % and detection limit about 10 % (Doelsch et al., 2006; Le Bars et al., 2018).

3. Results and discussion

3.1. Mineralogy of soil density fractions

The XRD characterization of the light, intermediate, and heavy fractions is shown in Fig. 1. For simplicity, only diffractograms for the PK-soil are shown, as the ones for the OW-soil were identical (Supporting Information SI-1). The heavy fraction contained the Fe and Ti oxides anatase (TiO_2, d = 3.89 g·cm^{-1}), rutile (TiO_2, d = 4.25 g·cm^{-3}), hematite (Fe_2O_3, d = 5.26 g·cm^{-3}), ilmenite ($FeTiO_3$, d = 4.79 g·cm^{-3}), and some undistinguished pyroxenes. The light and intermediate fractions showed ambiguous diffraction peaks centered at 14.2°2θ (7.2 Å) and 7.1°2θ (14.4 Å) that were further investigated by solvation in ethylene glycol and heating of the previously isolated clay fraction (Section 2.2). The peak centered at 14.2°2θ (7.2 Å) is attributed to the (001) reflection of kaolinite, as it disappeared upon heating at 490 °C (ruling out chlorite) and because the peak at 29.0°2θ (3.57 Å) indicated the (002) reflection of kaolinite (ruling out serpentine) (Dixon, 1989). The peak centered at 7.1°2θ (14.4 Å) is attributed to hydroxy-interlayered vermiculite, as it (a) did not shift to higher d spacing upon ethylene glycol solvation (ruling out smectite), and (b) broadened and shifted to 7.55°2θ (13.6 Å) and 8.3°2θ (12.4 Å) upon heating at, respectively, 300 °C and 490 °C (Harris et al., 1992; Meunier, 2007; Yin et al., 2013). Therefore, the intermediate fraction contained kaolinite [$Al_2Si_2O_5(OH)_4$, d = 2.63 g·cm^{-3}], vermiculite [$(Mg,Fe,Al)_3(Al,Si)_4O_{10}(OH)_2.4H_2O$, d = 2.50 g·$cm^{-3}$), quartz ($SiO_2$, d = 2.66 g·$cm^{-3}$), and traces of hematite and gibbsite [$Al(OH)_3$, d = 2.44 g·cm^{-3}]. Finally, the OM-rich (see Section 3.2) light fraction contained traces of kaolinite and vermiculite, most likely in the form of low-density organo-mineral aggregates (Badin et al., 2009; El-Mufleh et al., 2014), as supported by the diffusion bands centered around 24°2θ that may indicate OM and/or low-crystallized mineral phases (Bonnard et al., 2012).

3.2. Cu enrichment in the bulk OW-soil and its density fractions

Fig. 2 shows the distribution of Cu and TOC amongst the density fractions of the PK-soil and the OW-soil, compared with the bulk soils. These distributions were normalized to take into account the Cu and TOC extracted by the fractionation solution during the fractionation steps. The normalization procedure, together with non-normalized Cu and TOC concentrations are shown in Supporting Information SI-1.

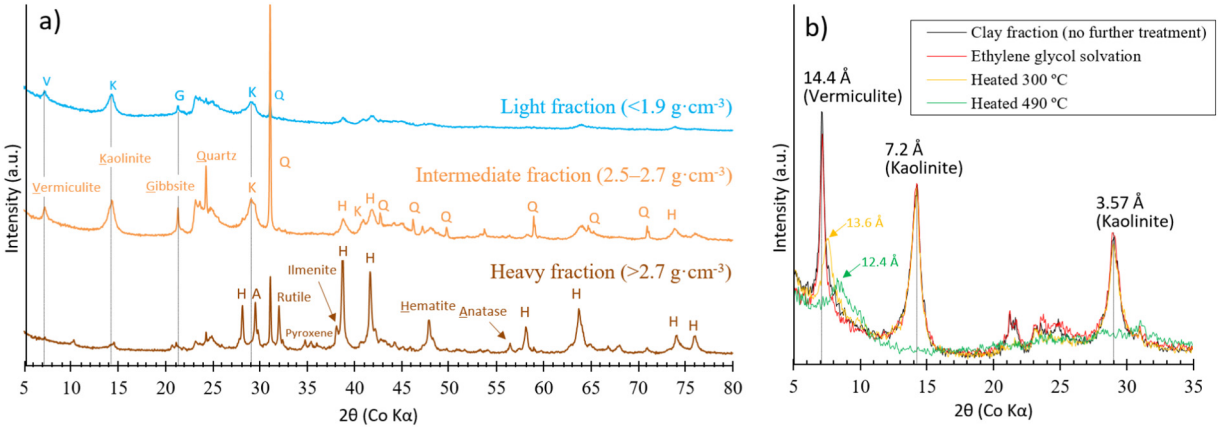

Fig. 1. (a) XRD diffractograms for the soil density fractions. The diffractograms for equivalent fractions (light, intermediate, and heavy) of different soils (PK- or OW-soil) were equivalent (Supporting Information SI-1). For simplicity, only the density fractions of the PK-soil are shown. (b) XRD diffractograms for the isolated clay fraction of the bulk PK-soil before and after ethylene glycol solvation and heating. This was used to confirm the presence of vermiculite and kaolinite in the soil.

The 0–5 cm layer of the bulk PK-soil had Cu at 122 mg·kg^{-1}, which increased to 174 mg·kg^{-1} in the bulk OW-soil amended with pig slurry. TOC increased from 43.2 mg·g^{-1} in the bulk PK-soil to 50.5 mg·g^{-1} in the bulk OW-soil (Fig. 2). The light fraction (<1.9 g·cm^{-3}) was rich in OM (as accessed by TOC). The light fraction of the PK-soil contained 12.5 mg Cu per kg of bulk soil ($mg_{Cu}{\cdot}kg_{bulk}^{-1}$), whereas the light fraction of the OW-soil contained 33.4 $mg_{Cu}{\cdot}kg_{bulk}^{-1}$ (Fig. 2). Therefore, the long-term application of organic waste (OW) caused an increase of 20.9 $mg_{Cu}{\cdot}kg_{bulk}^{-1}$ (or 167 %) in the Cu content within the light fraction, the most pronounced amongst density fractions. The intermediate fraction (2.5–2.7 g·cm^{-3}) was low in OM. The intermediate fraction of the PK-soil contained 90.2 $mg_{Cu}{\cdot}kg_{bulk}^{-1}$, whereas the intermediate fraction of the OW-soil contained 98.8 $mg_{Cu}{\cdot}kg_{bulk}^{-1}$ (Fig. 2). Therefore, the intermediate fraction of the OW-soil contained 10 % more Cu as in the PK-soil due to the OW applications. The heavy fraction (>2.7 g·cm^{-3}) did not contain OM. The heavy fraction of the PK-soil contained 7.8 $mg_{Cu}{\cdot}kg_{bulk}^{-1}$, whereas the heavy fraction of the OW-soil contained 7.1 $mg_{Cu}{\cdot}kg_{bulk}^{-1}$. Hence, no accumulation of exogenous Cu was apparent in the heavy fraction. However, its mineralogical composition was drastically different from the other fractions (Section 3.1) and thus the Cu speciation in this fraction was studied as well. The other fractions (1.9–2.25 and 2.25–2.5 g·cm^{-3}) held low proportions of Cu and were not sufficiently contrasting with the light fraction or with the intermediate fraction. For this reason, they were not further investigated using XAS.

3.3. XANES: evidence of Cu(I) sulfide in the pig slurry and octahedral Cu(II) surrounded by O in the soils

The Cu K-edge X-ray absorption near edge structure (XANES) spectra for the pig slurry, the bulk PK-soil, and the bulk OW-soil are compared in Fig. 3 with selected Cu reference compounds. The absorption edge energies E for the reference compounds occurred in the order E(Cu(II)) > E(Cu(I)) > E(Cu(0)), because electrons and nuclei interact more strongly in atoms with higher oxidation states (at comparable molecular environments). The rising-edge peak at ca. 8982 eV for Cu_2O (feature "a", Fig. 2) is assigned to 1 s-4p_x and 1 s-4p_y transitions occurring at lower energy than the 1 s-4p_z transition in this two-coordinate Cu(I) compound. The shoulder at ca. 8984 eV for CuO (feature "b", square-planar Cu(II)) and the shoulder at ca. 8986 eV for $Cu(OH)_2$ (feature "c", octahedral Cu(II)) are assigned to the 1 s-4p_z + shakedown transition.

The XANES spectra for the bulk PK-soil and the bulk OW-soil had shape and absorption edge energy similar to $Cu(OH)_2$, suggesting that Cu(II) in octahedral-like symmetry, surrounded by O atoms in the first coordination shell prevailed in both soils. The light fractions (LF in Fig. 3), intermediate fractions (IF) and heavy fractions (HF) had XANES fingerprint slightly different amongst each other, and also different from their bulk counterparts. These differences were further explored using EXAFS analysis (Sections 3.4 to 3.6). The XANES spectra for the pig slurry featured a distinctive rising-edge peak at 8986 eV (feature "d", Fig. 3), present in the XANES spectra for CuS and Cu_2S. This indicates that Cu(I) sulfide likely dominated the Cu speciation in the pig slurry (also explored using EXAFS in Section 3.6).

3.4. EXAFS: the intermediate fraction resembled the PK-soil and the light fraction resembled the OW-soil

The Cu K-edge EXAFS spectra and Fourier transforms (FT) for the bulk PK-soil, bulk OW-soil, their density fractions, and the pig slurry applied to the OW-soil are shown in Fig. 4. The spectra for the bulk PK-soil and bulk OW-soil were distinct in their first EXAFS oscillation that was split into two peaks for the PK-soil, but had only a shoulder for the OW-soil (double-line rectangles, Fig. 4a).

3.4.1. Light fractions

The EXAFS spectra for the PK-soil and OW-soil light fractions were similar, both having a shoulder before 3.85 Å^{-1} (solid-line rectangles, Fig. 4a). This shoulder was also present in the EXAFS spectrum for the bulk OW-soil.

3.4.2. Intermediate fractions

The EXAFS spectra for the intermediate fractions (PK-soil and OW-soil) were similar. The first oscillation was split into two peaks at about 3.85 Å^{-1} (dashed rectangles, Fig. 4a) as in the bulk PK-soil. The splitting at 3.85 Å^{-1} is uncommon in the Cu K-edge EXAFS spectra for soils and minerals. Indeed, the same feature appears only in a limited number of Cu reference compounds in the extensive library shown in Fig. S2, namely Cu-formate, Cu-acetate, $Cu(OH)_2$, $Cu_2(CO_3)(OH_2)$, and Cu-sorbed vermiculite (interlayer dimer). These Cu references have in common a central Cu coordinating with a second Cu atom, forming a Cu dimer. This Cu environment was further analyzed in Sections 3.5 and 3.6.

3.4.3. Heavy fractions

The EXAFS spectra for the heavy fractions (PK-soil and OW-soil) were similar to each other, but drastically different from the other fractions or from their bulk soil counterparts. This indicates that the molecular environment of Cu in the heavy fraction (i) drastically differed from that in the light and intermediate fractions, and (ii) accounted for only a small proportion of the overall Cu speciation in the bulk soils. The first EXAFS oscillation for the heavy fractions was centered slightly after 3.85 Å^{-1} (vertical dashed line, Fig. 4a). Moreover, the spectra showed high amplitude oscillations after 7 Å^{-1}, which is characteristic of neighboring atoms with higher atomic number Z that scatter photoelectrons more strongly at higher k-values (Kelly et al., 2008). The second FT peak (representing the second coordination shell of Cu) was more intense and at a higher distance (2.66 Å, vertical

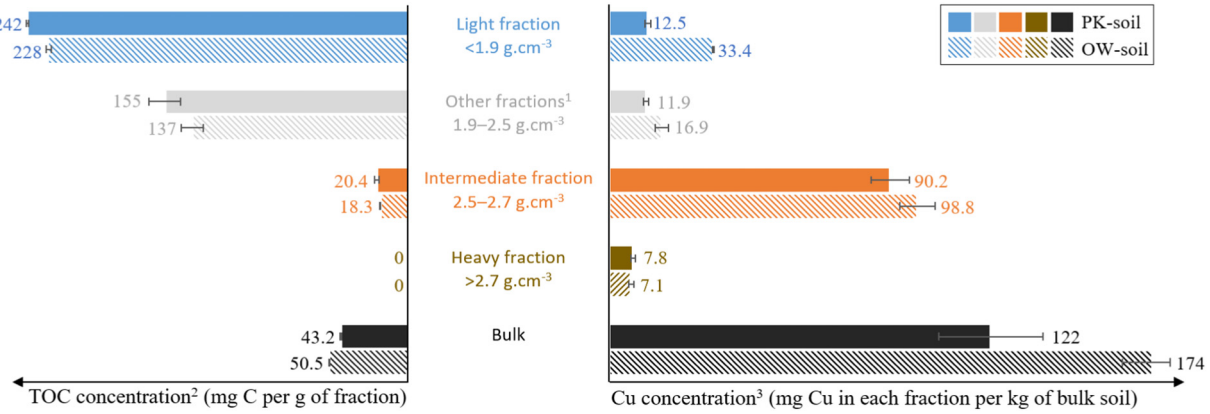

Fig. 2. Normalized Cu and TOC concentrations in the density fractions of the PK-soil and the OW-soil. [1]Other fractions are the sum of 1.9–2.25 g.cm^{-3} and 2.25–2.5 g.cm^{-3}, which were not further explored in this study (see text). [2]Unit for TOC is mg C per g of fraction or bulk, representing the concentration in each fraction or in the bulk. [3]Unit for Cu is mg Cu per kg of bulk soil, representing the concentration in each fraction proportionally to the bulk soil mass. The complete dataset is shown in Table S1.

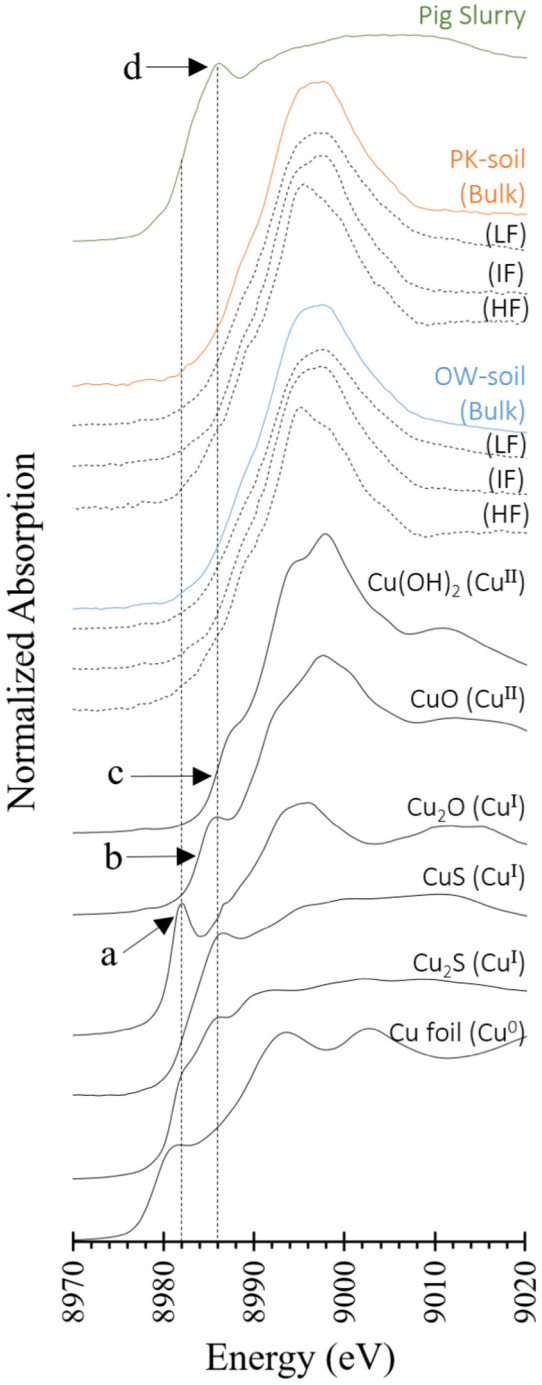

Fig. 3. Cu K-edge XANES spectra for the pig slurry, PK-soil, OW-soil and references containing Cu^0, Cu^I and Cu^{II} with different coordination and ligands. Features "a" to "d" are discussed in the text.

dashed line, Fig. 4b) in the heavy fractions, as compared to the light and intermediate fractions (2.58 Å, vertical dashed line, Fig. 4b). Likely Cu second neighbors within the heavy fractions are Fe and Ti, as this fraction was composed primarily of Fe and Ti oxides (Section 3.1). The Cu molecular environment in the heavy fraction was investigated using LCF (Section 3.6), as the library of Cu reference compounds used in LCF included Cu sorbed to Fe (hydr)oxides as well as Cu incorporated into the structure of Fe (hydr)oxides, both showing distinct spectral features (Supporting Information SI-2).

3.4.4. Pig slurry

The Cu K-edge EXAFS spectrum for the pig slurry applied to the OW-soil was markedly different, predominantly out of phase, as compared with the PK-soil, the OW-soil, and their density fractions. The first FT peak for the pig slurry was centered slightly after 1.8 Å (not phase shifted), that is longer than in the bulk soils and density fractions (ca. 1.42 Å, not phase shifted, Fig. 4b). Therefore, the first Cu neighbor in the pig slurry was likely a different element than in the soils, in line with XANES observations (Section 3.3) and further explored using LCF (Section 3.6).

3.5. Fourier filtering: the 3.85-$Å^{-1}$ splitting was caused by a heavy Cu neighbor

The EXAFS spectra for the intermediate fractions (PK-soil and OW-soil) shared features with the bulk PK-soil whereas the EXAFS spectra for the light fractions (PK-soil and OW-soil) were similar to the bulk OW-soil (Section 3.4). Fourier filtering was used to explore the molecular environment of Cu in these fractions. Fig. 5a shows that the first FT peak occurred at the same distance for the light fraction and for the intermediate fraction (not phase shifted; vertical dashed line labeled "1.42 Å"). The back transformed wavelet for the 1.42 Å peak in both fractions had high amplitude and low frequency (brown oscillations, Fig. 5b), typical for scattering paths from short-distance neighbors. Therefore, the light fraction and the intermediate fraction probably had the same (light) element in the first Cu coordination shell.

The second FT peaks, however, were centered at different distances for the light and for the intermediate fractions. The FT peak at ca. 2.58 Å for the intermediate fraction (not phase shifted; vertical dashed line labeled "2.58 Å" in Fig. 5a) was rather intense, suggesting a heavy element in the second coordination shell such as Fe, Ti or another Cu. The back transformed wavelet for this shell (blue oscillation, Fig. 5b, top) reached a minimum at 3.85 $Å^{-1}$ (vertical dashed line labeled "3.85 $Å^{-1}$") that is perfectly in phase with the splitting of the first oscillation in (i) the EXAFS spectrum reconstructed using backscatter wavelets (black spectra, Fig. 5b, top) and (ii) the experimental EXAFS spectrum for the intermediate fraction (red spectra overlapped). This indicates that the splitting in the first EXAFS oscillation at 3.85 $Å^{-1}$ (the uncommon spectral feature of the intermediate fraction and the bulk PK-soil) was caused by interference between scattering paths from the first (light) and second (heavy) Cu neighbors. LCF was used to identify and quantify the Cu species in the bulk soils, density fractions, and in the pig slurry (presented next in Section 3.6).

3.6. LCF: the resulting Cu speciation in the bulk soils, density fractions, and pig slurry

The library of Cu reference compounds, for which different XAS spectral features are presented and discussed in Supporting Information SI-2 and Fig. S2, was utilized in LCF to determine the Cu speciation in the bulk soils, in the density fractions, and in the pig slurry applied to the OW-soil. Overlaps between experimental and LCF-derived EXAFS spectra and FT, with the corresponding residual factors R, are shown in Fig. S3.

3.6.1. Bulk PK-soil and fractions

The bulk PK-soil had 54 % Cu-vermiculite (interlayer dimer) and 46 % Cu-kaolinite (Fig. 6). In Cu-kaolinite, Cu was bonded to the edges of the clay layer as an inner-sphere complex, sharing edges with Al octahedral (Schlegel and Manceau, 2013). In Cu-vermiculite, Furnare et al. (2005) proposed that reduction of structural Fe(III) in the octahedral sheets of vermiculite increases the negative interlayer charge, allowing cations such as Cu to overcome the hydration energy and replace weakly held axial ligands, forming dimeric Cu structures in the interlayer [see Fig. 9 in Furnare et al., 2005]. This can explain Cu-vermiculite (interlayer dimer) dominating the Cu speciation in the PK-soil, that is the soil containing natural Cu. Interlayered clays such as vermiculite often display great stability in natural soil environments, although the degree of stability may vary depending on system specificities and interlayer occupancy (Singh and Schulze, 2015). Indeed, over 70 % of Cu in the bulk PK-soil (the same soil studied here)

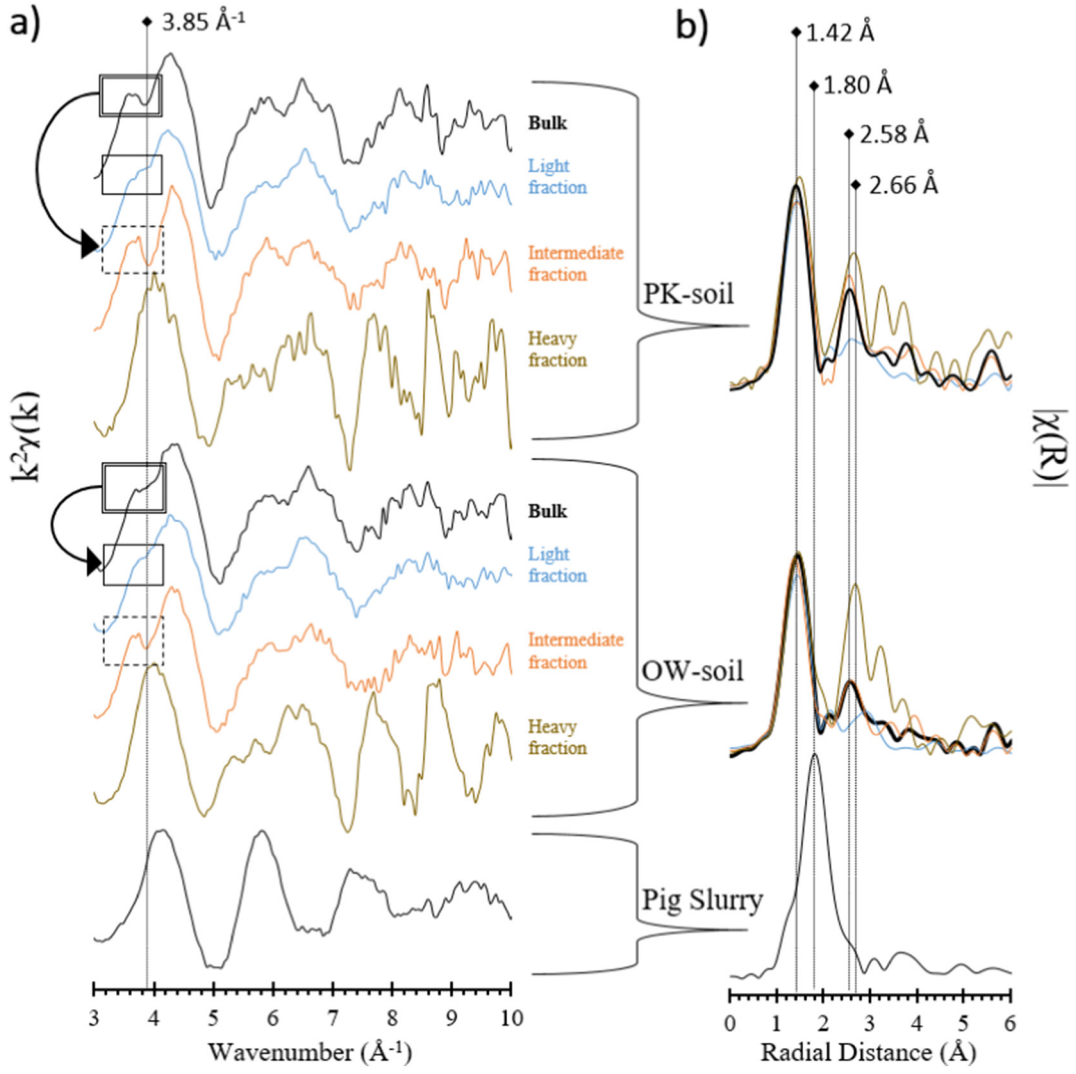

Fig. 4. (a) k^2-weighted Cu k-edge EXAFS spectra and (b) Fourier transforms (FT, uncorrected for phase shift functions) for the bulk PK-soil, bulk OW-soil, their density fractions, and pig slurry. The EXAFS spectra in "a" are offset to highlight the features around 3.85 $Å^{-1}$. The FT for each soil and their density fractions in "b" are overlapped to compare the intensity of FT peaks representing Cu neighbors.

was in the residual fraction of a sequential extraction scheme (Formentini et al., 2015), only accessible when the soil was subjected to microwave-assisted acid digestion.

The PK-soil intermediate fraction was fitted with 75 % Cu-vermiculite (interlayer dimer) and 25 % Cu-kaolinite. This confirms the spectral resemblance between the intermediate fraction and the bulk PK-soil (Fig. 4), reinforcing that Cu-vermiculite (interlayer dimer) was the major Cu species in the PK-soil. LCF analysis also revealed low-proportion Cu species within the PK-soil light and heavy fractions that could not be detected looking at the bulk PK-soil only. The PK-soil light fraction was fitted with 83 % Cu-kaolinite and 17 % Cu-OM. Finally, the PK-soil heavy fraction was an excellent match with the EXAFS for Cu-substituted hematite, as this was the only reference (100 %) required to successfully fit the heavy fraction (Fig. 6, Fig. S3).

In Cu-hematite, Cu was uniformly distributed within the crystalline structure, with Jahn-Teller distorted Cu(II) located within an Fe(III) octahedral site (Frierdich and Catalano, 2012). Redox-driven dynamic recrystallization of Fe oxides (e.g. hematite) during pedogenesis, which presumably occurs via oxidative adsorption of Fe(II) coupled to reductive dissolution of Fe(III), caused speciation changes in redox-active (i.e. Cu) and redox-inactive (e.g. Ni) trace elements (Frierdich and Catalano, 2012; Frierdich et al., 2011). Such cycling may impact the incorporation or release of Cu from the Cu-substituted hematite observed in the heavy fraction. The Cu structurally incorporated within hematite should be extremely recalcitrant under static oxidizing conditions, as hematite is one of the most stable Fe (III) oxides found in soils (Barnhisel and Bertsch, 1989).

3.6.2. Pig slurry

Cu in the pig slurry applied to the OW-soil causing approximately 50 % increase in the Cu concentration was composed of 100 % Cu(I) sulfide (best reference: Cu_2S, Fig. 6, Fig. S3). This is consistent with the anoxic environment in the lagoon that provided the pig slurry applied to the OW-soil. Noteworthy, the Zn speciation in the same pig slurry consisted of 100 % ZnS (Formentini et al., 2017). Cu(I) sulfides have been observed as a major component (>90 %) in pig slurry (Legros et al., 2010) and at relatively lower proportions also in pig slurry (16–23 %), municipal waste fine fraction (29–49 %), sewage sludge (42–51 %) (Legros et al., 2017), biosolids (27–60 %) (Donner et al., 2011), and swine manure (30–69 %) (Cheng et al., 2020). The higher proportion (100 %) of Cu(I) sulfide found in pig slurry here is attributed to the special care taken to preserve the sample anaerobic conditions during sampling, storage, and analysis (Section 2.1).

Although Cu(I) sulfide accounted for 100 % of the Cu speciation in the pig slurry, this species was not detected neither in the bulk nor in the density fractions of the OW-soil [sensitivity of EXAFS LCF for minor species is estimated at 10 % (Doelsch et al., 2006)]. The density of bulk Cu_2S is

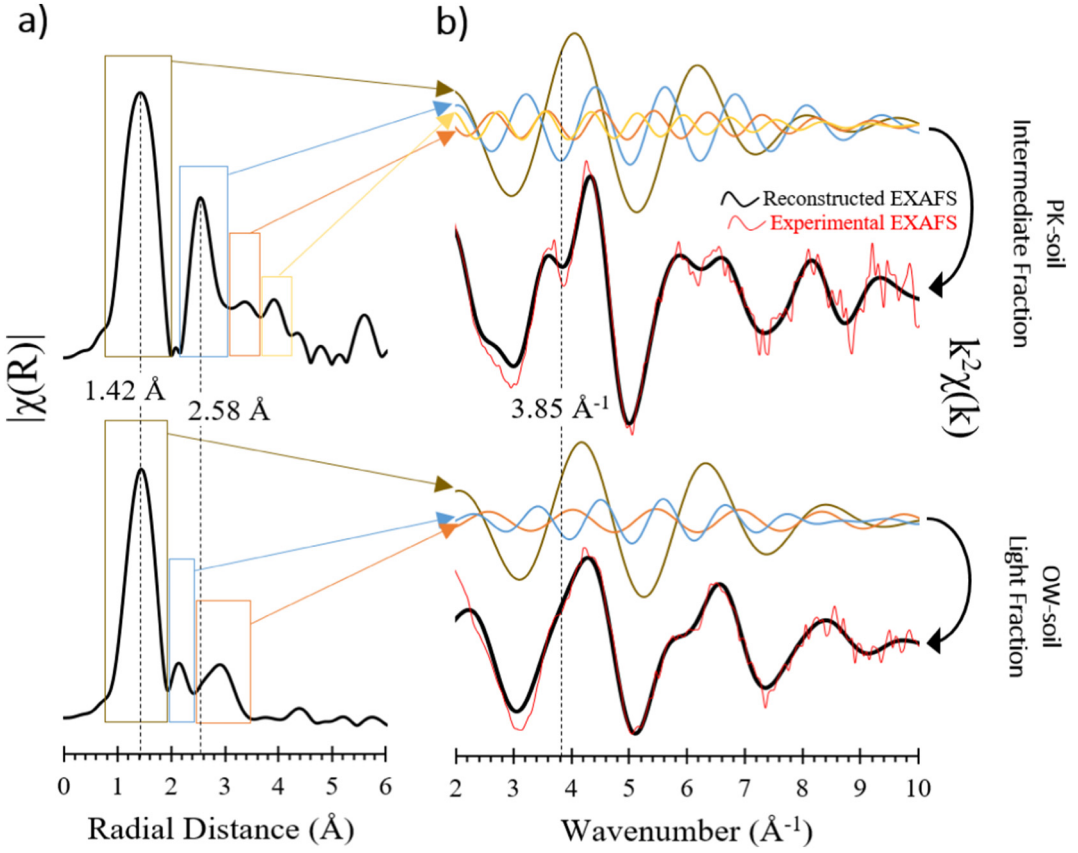

Fig. 5. (a) Fourier transforms (FT, uncorrected for phase shift functions) were back transformed to obtain (b) backscatter wavelets for each Cu coordination shell. The EXAFS spectra were then reconstructed (black lines in "b") combining the individual backscatter wavelets and overlapped with the experimental EXAFS spectra (red lines in "b"). This approach demonstrates that the splitting of the first EXAFS oscillation at 3.85 $Å^{-1}$ for the intermediate fraction (vertical dashed line in "b") was caused by destructive interference between single scattering paths for the first (brown line) and second (blue line) Cu coordination shells.

5.6 $g.cm^{-3}$, within the range of the heavy fraction (>2.7 $g.cm^{-3}$) that contained 7.1 mg of Cu per kg of bulk OW-soil (Fig. 5). The absence of Cu (I) sulfide in the heavy fraction (at 10 % LCF sensitivity) implies that Cu (I) sulfide accounted, if any, for <0.71 mg per kg of bulk OW-soil. Since the Cu concentration increased 52 $mg.kg^{-1}$ over 11 years due to pig slurry amendments (average 4.7 $mg.kg^{-1}.year^{-1}$), it is safe to assume that the depletion of Cu(I) sulfide occurred in less than six months, that was the interval between the last pig slurry application and the soil sampling. This is

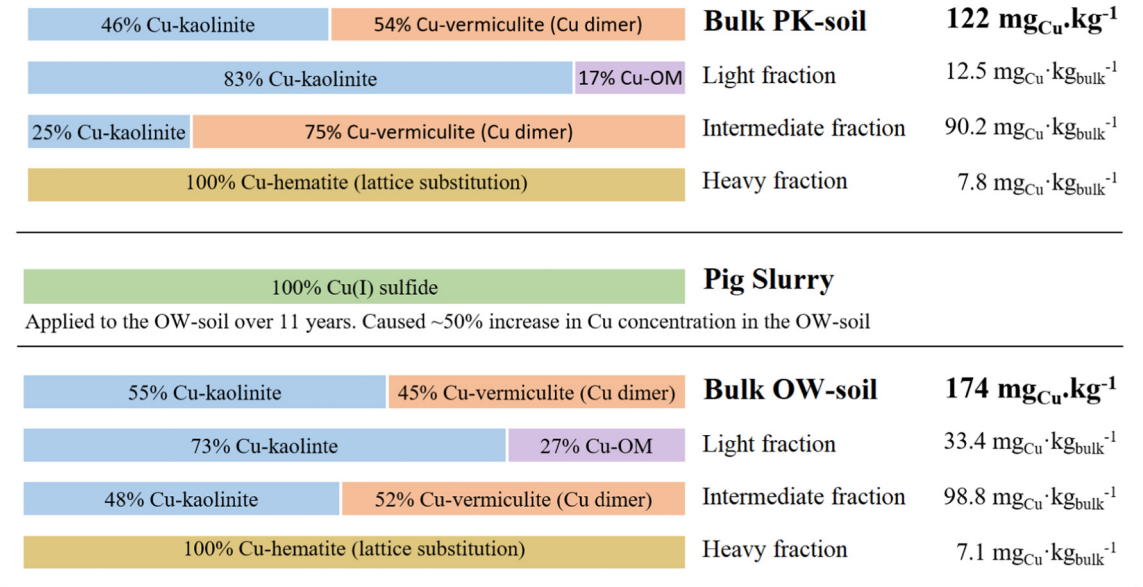

Fig. 6. LCF-derived Cu species in the PK-soil and its density fractions, in the pig slurry that was applied to the OW-soil over 11 years, and in the OW-soil and its density fractions. LCF spectra are presented in Supporting Information SI-2.

reinforced by the fact that the heavy fraction was the only density fraction with no Cu increase due to application of Cu(I)-sulfide-rich pig slurry (Fig. 2).

The rapid depletion of pig-slurry-borne Cu(I) sulfide is surprising given the chemical stability of bulk Cu_2S, which has very low solubility product constant ($K_{sp} = 2.5 \times 10^{-48}$) (Spencer et al., 2010). Zhou et al. (1999) showed that the solubility of Cu sulfides in soil under aerobic conditions was very low in the 6.6–7.6 pH range. Calmano et al. (1993) reported that Cu sulfides were soluble in oxidized sediment only at pH < 4.5, with limited influence of redox conditions. For comparison, the pH of the soil analyzed in the present study was 5.8 (Veiga et al., 2012). On the other hand, nanoparticles are considered less stable (i.e. dissolve more quickly) than their bulk counterparts due to their small size (Auffan et al., 2009; Mudunkotuwa and Grassian, 2011). Therefore, Cu(I) sulfide found in the present study was most likely nano sized, and its oxidative dissolution can explain the change in Cu speciation after soil amendments. This could also explain why Cu_2S did not persist in biosolids when the conditions changed from reducing (fresh biosolids) to oxidizing (stockpiled biosolids) (Donner et al., 2011), although information or discussion on particle size was not provided.

Zinc sulfide (ZnS, $K_{sp} = 2.93 \times 10^{-36}$) has also been reported in pig slurry, and the nano size of the ZnS particles explained the low stability in the soil (Formentini et al., 2017). Recently, Le Bars et al. (2022) showed fast dissolution of nano ZnS in clayey soil (82 % within 1 month) in controlled incubation experiments. Similar to Cu, these results were contrasting with the low solubility of bulk ZnS (63-μm crystals) in soils, for which dissolution rates of ranged from only 0.6 % to 1.2 % within one year (Robson et al., 2014). The influence of the particle size on the solubility, fate and toxicity of nano-structured Cu(I) sulfide in the soils requires further research.

3.6.3. Bulk OW-soil and fractions

The bulk OW-soil contained 45 % Cu-vermiculite (interlayer dimer) and 55 % Cu-kaolinite (Fig. 6). Compared to the bulk PK-soil, the proportion of Cu-kaolinite in the OW-soil was higher and the proportion of Cu-vermiculite was lower. This indicates that kaolinite contributed the most to sorb the OW-borne Cu after dissolution of Cu(I) sulfides, although the natural Cu associated with vermiculite persisted in the OW-soil. LCF analysis of the OW-soil density fractions revealed other Cu species at lower proportions. The OW-soil light fraction contained 73 % Cu-kaolinite and 27 % Cu bound to OM. The OW-soil intermediate fraction had 52 % Cu-vermiculite (interlayer dimer) and 48 % Cu-kaolinite. The OW-soil heavy fraction contained 100 % Cu-substituted hematite (Fig. 6, Fig. S3).

Therefore, Cu-kaolinite was the species that increased more markedly in the OW-soil. The Cu-kaolinite reference used to fit the EXAFS spectra for the OW-soil and its density fractions (Schlegel and Manceau, 2013) had Cu sorbed in an inner-sphere, edge-sharing fashion with Al octahedra. Indeed, Cu showed very good size and bond-angle match with Al octahedra in dioctahedral structures (Petit et al., 1995). On the other hand, the geometry of the Cu(II) coordination polyhedron makes Cu less compatible to replace Al(III) and bond with Mg octahedra in trioctahedral clays such as vermiculite (Schlegel and Manceau, 2013). This explains why newly solubilized pig-slurry-borne Cu was sorbed on the surface of kaolinite in the OW-soil, whereas Cu in the PK-soil occurred mostly as a Cu dimer in the interlayer of vermiculite, likely involving long-term processes along pedogenesis.

Detecting kaolinite in the light fraction (Section 3.1) was likely due to the formation of organo-mineral aggregates that lowered the density of pure kaolinite (2.6 $g{\cdot}cm^{-3}$) down to the density range of the light fraction (<1.9 $g{\cdot}cm^{-3}$), as already reported elsewhere (Badin et al., 2009; Bonnard et al., 2012; El-Mufleh et al., 2014). Organo-mineral associations such as kaolinite-fulvic acid (Heidmann et al., 2005) and kaolinite-humic acid (Arias et al., 2002; Komy et al., 2014) enhanced the sorption capacity towards Cu as compared to pure mineral systems. Alcacio et al. (2001) showed that Cu formed bridge-like bonds in between goethite and OM in goethite–humic mixtures at a narrow mineral-to-OM ratio. Here, no direct XAS evidence for Cu bridging with OM and mineral ligands in the OW-soil was found. However, it cannot be ruled out that Cu was either sorbed to kaolinite that was itself bound to OM (i.e. a Cu-kaolinite-OM complex) or bound to OM that was itself bound to kaolinite (i.e. a Cu-OM-kaolinite complex). This could explain the OW-soil light fraction accounting for higher uptake of exogenous Cu yet kaolinite (the major Cu bearing phase in the bulk OW-soil) was more abundant in the intermediate fraction. Further investigation may reveal the mechanisms that promote the increase in the sorption capacity for Cu-organo-mineral complexes.

3.7. Environmental implications

Natural Cu inherited from parent rock, that is Cu present in the PK-soil (no pig slurry amendments) was 55 % in the form of a Cu dimer in the interlayer of vermiculite. At lower proportions, natural Cu was also structurally incorporated within hematite. To the best of our knowledge, neither of these molecular environments of Cu in soils have been reported previously. This might well be the case in different soils throughout the world, which can only be elucidated with further research. A better understanding on the fate of potential soil contaminants such as Cu benefits from a comprehensive characterizations of its pristine forms too.

Cu(I) sulfide, which accounted for 100 % of the Cu speciation in the pig slurry, was not present in the OW-amended soil. Cu(I) sulfide at such dominant proportion in livestock wastes has not been reported previously either. It might also be the prevailing species in most organic wastes subject to anaerobic conditions, though this has been overlooked so far due to the little care taken in preserving these conditions along sampling and analysis. The fate of (nano) Cu(I) sulfides formed in organic wastes deserves more attention in soil–water–plant systems as very little has been studied on their formation, behavior and ecotoxicity.

The present study provided a molecular-scale description (with a drastic Cu speciation change) for the macroscopic behavior observed previously (Formentini et al., 2015), that is pig-slurry-borne Cu accumulating within soil surface after 11 years of amendments. With unchanged agricultural practices, Cu concentrations might keep increasing within the soil surface. Cu phytoavailability, leaching and runoff therefore pose a long-term risk if the clay (in this case, mostly kaolinite) sorption capacity is exceeded or in different soils where the sorption capacity is lower due to different e.g. pH, OM content, texture, or mineralogy. On the other hand, OM mineralization may release the Cu associated with this soil phase, which represents a short-term risk (Tella et al., 2016) that requires consideration to assess the overall environmental impacts of the agricultural recycling of organic waste.

CRediT authorship contribution statement

Thiago A. Formentini: Investigation, Formal analysis, Writing – original draft, Visualization. **Isabelle Basile-Doelsch:** Methodology, Writing – review & editing, Supervision. **Samuel Legros:** Investigation, Validation, Formal analysis, Writing – review & editing. **Andrew J. Frierdich:** Writing – review & editing. **Adilson Pinheiro:** Conceptualization, Writing – review & editing, Supervision, Project administration. **Cristovão V.S. Fernandes:** Writing – review & editing, Supervision, Funding acquisition. **Fábio J.K. Mallmann:** Investigation, Resources, Writing – review & editing. **Daniel Borschneck:** Investigation, Resources. **Milton da Veiga:** Methodology, Investigation, Resources. **Emmanuel Doelsch:** Conceptualization, Methodology, Formal analysis, Investigation, Writing – review & editing, Funding acquisition.

Data availability

Data will be made available on request.

Declaration of competing interest

The authors declare that they have no known competing financial interests or personal relationships that could have appeared to influence the work reported in this paper.

Acknowledgments

We are grateful to Copercampos for authorizing this study in its experimental area; Epagri for providing the soil samples; the European Synchrotron Radiation Facility (ESRF) for providing access to the synchrotron radiation facilities; Isabelle Kiefer for assistance in using beamline BM 30 FAME; Bernard Angeletti for ICP-MS assistance; and Daniel Strawn for providing the Cu-vermiculite XAS reference. T.A. Formentini acknowledges CAPES for a postgraduate scholarship (99999.000142/2014-00) and UFSM for the leave of absence. Abstract art created with BioRender.

Appendix A. Supplementary data

Supplementary data to this article can be found online at https://doi.org/10.1016/j.scitotenv.2022.157779.

References

Alcacio, T.E., Hesterberg, D., Chou, J.W., Martin, J.D., Beauchemin, S., Sayers, D.E., 2001. Molecular scale characteristics of Cu(II) bonding in goethite–humate complexes. Geochim. Cosmochim. Acta 65 (9), 1355–1366. https://doi.org/10.1016/s0016-7037(01)00546-4.

Arias, M., Barral, M.T., Mejuto, J.C., 2002. Enhancement of copper and cadmium adsorption on kaolin by the presence of humic acids. Chemosphere 48 (10), 1081–1088. https://doi.org/10.1016/s0045-6535(02)00169-8.

Auffan, M., Rose, J., Bottero, J.-Y., Lowry, G.V., Jolivet, J.-P., Wiesner, M.R., 2009. Towards a definition of inorganic nanoparticles from an environmental, health and safety perspective. Nat. Nanotechnol. 4 (10), 634–641. https://doi.org/10.1038/nnano.2009.242.

Badin, A.L., Méderel, G., Béchet, B., Borschneck, D., Delolme, C., 2009. Study of the aggregation of the surface layer of technosols from stormwater infiltration basins using grain size analyses with laser diffractometry. Geoderma 153, 163–171. https://doi.org/10.1016/j.geoderma.2009.07.022.

Barnhisel, R.I., Bertsch, P.M., 1989. Chlorites and hydroxy-interlayered vermiculite and smectite. In: Dixon, J.B., Weed, S.B. (Eds.), Minerals in Soil Environments, 2nd editionThe Soil Science Society of America Book Series, Madison, Wisconsin, pp. 729–788.

Bonnard, P., Basile-Doelsch, I., Balesdent, J., Masion, A., Borschneck, D., Arrouays, D., 2012. Organic matter content and features related to associated mineral fractions in acid loamy soil. Eur. J. Soil Sci. 63 (5), 625–636. https://doi.org/10.1111/j.1365-2389.2012.01485.x.

Boudesocque, S., Guillon, E., Aplincourt, M., Marceau, E., Stievano, L., 2007. Sorption of Cu (II) onto vineyard soils: macroscopic and spectroscopic investigations. J. Colloid Interface Sci. 307 (1), 40–49. https://doi.org/10.1016/j.jcis.2006.10.080.

Calmano, W., Hong, J., Förstner, U., 1993. Binding and mobilization of heavy metals in contaminated sediments affected by pH and redox potential. Water Sci. Technol. 28 (8–9), 233–235. https://doi.org/10.2166/wst.1993.0622.

Cheng, Y., Luo, L., Lv, J., Li, G., Wen, B., Ma, Y., Huang, R., 2020. Copper speciation evolution in swine manure induced by pyrolysis. Environ. Sci. Technol. 54 (14), 9008–9014. https://doi.org/10.1021/acs.est.9b07332.

Davidson, C.M., Ferreira, P.C.S., Ure, A.M., 1999. Some sources of variability in application of the three-stage sequential extraction procedure recommended by BCR to industrially-contaminated soil. Fresenius J. Anal. Chem. 363 (5–6), 446–451. https://doi.org/10.1007/s002160051220.

Dixon, J.B., 1989. Kaolin and serpentine group minerals. In: Dixon, J.B., Weed, S.B. (Eds.), Minerals in Soil Environments, 2nd ed. SSSA, pp. 467–525 https://doi.org/10.2136/sssabookser1.2ed.c10.

Doelsch, E., Basile-Doelsch, I., Rose, J., Masion, A., Borschneck, D., Hazemann, J.L., Macary, H.S., Bottero, J.Y., 2006. New combination of EXAFS spectroscopy and density fractionation for the speciation of chromium within an andosol. Environ. Sci. Technol. 40 (24), 7602–7608. https://doi.org/10.1021/es060906q.

Donner, E., Howard, D.L., de Jonge, M.D., Paterson, D., Cheah, M.H., Naidu, R., Lombi, E., 2011. X-ray absorption and micro X-ray fluorescence spectroscopy investigation of copper and zinc speciation in biosolids. Environ. Sci. Technol. 45 (17), 7249–7257. https://doi.org/10.1021/es201710z.

Edmonds, M.S., Izquierdo, O.A., Baker, D.H., 1985. Feed additive studies with newly weaned pigs: efficacy of supplemental copper, antibiotics and organic acids. J. Anim. Sci. 60 (2), 462–469. https://doi.org/10.2527/jas1985.602462x.

El-Mufleh, A., Béchet, B., Basile-Doelsch, I., Geffroy-Rodier, C., Gaudin, A., Ruban, V., 2014. Distribution of PAHs and trace metals in urban stormwater sediments: combination of density fractionation, mineralogy and microanalysis. Environ. Sci. Pollut. Res. 21, 9764–9776. https://doi.org/10.1007/s11356-014-2850-7.

Flogeac, K., Guillon, E., Aplincourt, M., 2004. Surface complexation of Copper(II) on soil particles: EPR and XAFS studies. Environ. Sci. Technol. 38 (11), 3098–3103. https://doi.org/10.1021/es049973f.

Formentini, T.A., Mallmann, F.J.K., Pinheiro, A., Fernandes, C.V.S., Bender, M.A., Veiga, M., dos Santos, D.R., Doelsch, E., 2015. Copper and zinc accumulation and fractionation in a clayey hapludox soil subject to long-term pig slurry application. Sci. Total Environ. 536, 831–839. https://doi.org/10.1016/j.scitotenv.2015.07.110.

Formentini, T.A., Legros, S., Fernandes, C.V.S., Pinheiro, A., Le Bars, M., Levard, C., Mallmann, F.J.C., Veiga, M., Doelsch, E., 2017. Radical change of zn speciation in pig slurry amended soil : key role of nano-sized sulfide particles. Environ. Pollut. 222, 495–503. https://doi.org/10.1016/j.envpol.2016.11.056.

Formentini, T.A., Basile-Doelsch, I., Borschneck, D., Venzon, J.S., Pinheiro, A., Fernandes, C.S.V., Mallmann, F.J.K., Veiga, M., Doelsch, E., 2021. Redistribution of zn towards light-density fractions and potentially mobile phases in a long-term manure-amended clayey soil. Geoderma 394 (1), 115044. https://doi.org/10.1016/j.geoderma.2021.115044.

Frierdich, A.J., Catalano, J.G., 2012. Fe(II)-mediated reduction and repartitioning of structurally incorporated cu co, and mn in iron oxides. Environ. Sci. Technol. 46 (20), 11070–11077. https://doi.org/10.1021/es302236v.

Frierdich, A.J., Luo, Y., Catalano, J.G., 2011. Trace element cycling through iron oxide minerals during redox-driven dynamic recrystallization. Geology 39 (11), 1083–1086. https://doi.org/10.1130/g32330.1.

Furnare, L.J., Vailionis, A., Strawn, D.G., 2005. Molecular-level investigation into copper complexes on vermiculite: effect of reduction of structural iron on copper complexation. J. Colloid Interface Sci. 289 (1), 1–13. https://doi.org/10.1016/j.jcis.2005.03.068.

Harris, W.G., Hollien, K.A., Bates, S.R., Acree, W.A., 1992. Dehydration of hydroxy-interlayered vermiculite as a function of time and temperature. Clay Clay Miner. 40 (3), 335–340. https://doi.org/10.1346/CCMN.1992.0400314.

Heidmann, I., Christl, I., Kretzschmar, R., 2005. Sorption of cu and pb to kaolinite-fulvic acid colloids: assessment of sorbent interactions. Geochim. Cosmochim. Acta 69 (7), 1675–1686. https://doi.org/10.1016/j.gca.2004.10.002.

Kelly, S.D., Hesterberg, D., Ravel, B., 2008. Analysis of soils and minerals using X-ray absorption spectroscopy. Methods of Soil Analysis Part 5—Mineralogical Methods, pp. 387–463.

Komy, Z.R., Shaker, A.M., Heggy, S.E.M., El-Sayed, M.E.A., 2014. Kinetic study for copper adsorption onto soil minerals in the absence and presence of humic acid. Chemosphere 99, 117–124. https://doi.org/10.1016/j.chemosphere.2013.10.048.

Le Bars, M., Legros, S., Levard, C., Chaurand, P., Tella, M., Rovezzi, M., Browne, P., Rose, J., Doelsch, E., 2018. Drastic change in zinc speciation during anaerobic digestion and composting: instability of nanosized zinc sulfide. Environ. Sci. Technol. 52 (22), 12987–12996. https://doi.org/10.1021/acs.est.8b02697.

Le Bars, M., Legros, S., Levard, C., Chevassus-Rosset, C., Montes, M., Tella, M., Borschneck, D., Guihou, A., Angeletti, B., Doelsch, E., 2022. Contrasted fate of zinc sulfide nanoparticles in soil revealed by a combination of X-ray absorption spectroscopy, diffusive gradient in thin films and isotope tracing. Environ. Pollut. 292 (B), 118414. https://doi.org/10.1016/j.envpol.2021.118414.

Legros, S., Chaurand, P., Rose, J., Masion, A., Briois, V., Ferrasse, J.-H., Doelsch, E., 2010. Investigation of copper speciation in pig slurry by a multitechnique approach. Environ. Sci. Technol. 44 (18), 6926–6932. https://doi.org/10.1021/es101651w.

Legros, S., Levard, C., Marcato-Romain, C.-E., Guiresse, M., Doelsch, E., 2017. Anaerobic digestion alters copper and zinc speciation. Environ. Sci. Technol. 51 (18), 10326–10334. https://doi.org/10.1021/acs.est.7b01662.

Mamindy-Pajany, Y., Sayen, S., Mosselmans, J.F.W., Guillon, E., 2014. Copper, nickel and zinc speciation in a biosolid-amended soil: PH adsorption edge, μ-XRF and μ-XANES investigations. Environ. Sci. Technol. 48 (13), 7237–7244. https://doi.org/10.1021/es5005522.

Manceau, A., Matynia, A., 2010. The nature of cu bonding to natural organic matter. Geochim. Cosmochim. Acta 74 (9), 2556–2580. https://doi.org/10.1016/j.gca.2010.01.027.

McBride, M.B., Bouldin, D.R., 1984. Long-term reactions of Copper(II) in a contaminated calcareous soil. Soil Sci. Soc. Am. J. 48 (1), 56. https://doi.org/10.2136/sssaj1984.03615995004800010010.

McBride, M.B., MartÍnez, C.E., 2000. Copper phytotoxicity in a contaminated soil: remediation tests with adsorptive materials. Environ. Sci. Technol. 34 (20), 4386–4391. https://doi.org/10.1021/es0009931.

McBride, M., Sauve, S., Hendershot, W., 1997. Solubility control of cu, zn, cd and pb in contaminated soils. Eur. J. Soil Sci. 48 (2), 337–346. https://doi.org/10.1111/j.1365-2389.1997.tb00554.x.

Meunier, A., 2007. Soil hydroxy-interlayered minerals: a re-interpretation of their crystallochemical properties. Clay Clay Miner. 55 (4), 380–388. https://doi.org/10.1346/CCMN.2007.0550406.

Mudunkotuwa, I.A., Grassian, V.H., 2011. The devil is in the details (or the surface): impact of surface structure and surface energetics on understanding the behavior of nanomaterials in the environment. J. Environ. Monit. 13 (5), 1135–1144. https://doi.org/10.1039/c1em00002k.

Paradelo, M., Moldrup, P., Arthur, E., Naveed, M., Holmstrup, M., López-Periago, J.E., de Jonge, L.W., 2013. Effects of past copper contamination and soil structure on copper leaching from soil. J. Environ. Qual. 42 (6), 1852. https://doi.org/10.2134/jeq2013.05.0209.

Petit, S., Decarreau, A., Mosser, C., Ehret, G., Grauby, O., 1995. Hydrothermal synthesis (250 °C) of copper-substituted kaolinites. Clay Clay Miner. 43, 482–494.

Ramos, L., Hernandez, L.M., Gonzalez, M.J., 1994. Sequential fractionation of copper, lead, cadmium and zinc in soils from or near Doñana National Park. J. Environ. Qual. 23 (1), 50. https://doi.org/10.2134/jeq1994.00472425002300010009x.

Ravel, B., Newville, M., 2005. ATHENA, ARTEMIS, HEPHAESTUS: data analysis for X-ray absorption spectroscopy using IFEFFIT. J. Synchrotron Radiat. 12 (4), 537–541.

Robson, T.C., Braungardt, C.B., Rieuwerts, J., Worsfold, P., 2014. Cadmium contamination of agricultural soils and crops resulting from sphalerite weathering. Environ. Pollut. 184, 283–289. https://doi.org/10.1016/j.envpol.2013.09.001.

Schlegel, M.L., Manceau, A., 2013. Binding mechanism of Cu(II) at the clay–water interface by powder and polarized EXAFS spectroscopy. Geochim. Cosmochim. Acta 113, 113–124. https://doi.org/10.1016/j.gca.2013.03.019.

Singh, B., Schulze, D.G., 2015. Soil minerals and plant nutrition. Nat. Educ. Knowl. 6 (1), 1.

Spencer, J.N., Bodner, G.M., Rickard, L.H., 2010. Chemistry: Structure and Dynamics. 5th edition. John Wiley & Sons 928 p. ISBN 0470587113, 9780470587119.

Strawn, D.G., Baker, L.L., 2009. Molecular characterization of copper in soils using X-ray absorption spectroscopy. Environ. Pollut. 157 (10), 2813–2821. https://doi.org/10.1016/j.envpol.2009.04.018.

Tella, M., Bravin, M.N., Thuriès, L., Cazevieille, P., Chevassus-Rosset, C., Collin, B., Doelsch, E., 2016. Increased zinc and copper availability in organic waste amended soil potentially involving distinct release mechanisms. Environ. Pollut. 212, 299–306. https://doi.org/10.1016/j.envpol.2016.01.077.

Ure, A.M., Davidson, C.M., Thomas, R.P., 1995. Single and sequential extraction schemes for trace metal speciation in soil and sediment. Tech. Instrum. Anal. Chem. 17, 505–523. https://doi.org/10.1016/S0167-9244(06)80021-1.

USDA – United States Department of Agriculture, 2003. Soil Survey Staff, Keys to Soil Taxonomy. 9th ed. Natural Resources Conservation Service, USDA, Washington.

USEPA – United States Environmental Protection Agency, 2007. Method 3051A: microwave assisted acid digestion of sediments, sludges, soils, and oils. Sw-846 Test Methods for Evaluation Solid Waste: Physical/chemical Methods. Washington.

Veiga, M., Pandolfo, C.M., Junior, A.A.B., Spagnollo, E., 2012. Chemical attributes of a hapludox soil after nine years of pig slurry application. Pesq. Agrop. Brasileira 47, 1766–1773. https://doi.org/10.1590/S0100-204X2012001200013.

Vincevica-Gaile, Z., Klavins, M., 2012. Transfer of metals in food chain: an example with copper and lettuce. Environ. Clim. Technol. 10, 21–24. https://doi.org/10.2478/v10145-012-0021-y.

Yamamoto, K., Hashimoto, Y., Kang, J., Kobayashi, K., 2018. Speciation of phosphorus zinc and copper in soil and water-dispersible colloid affected by a long-term application of swine manure compost. Environ. Sci. Technol. 52 (22), 13270–13278. https://doi.org/10.1021/acs.est.8b02823.

Yang, X.-E., Long, X.-X., Ni, W.-Z., Ye, Z.-Q., He, Z.-L., Stoffella, P.J., Calvert, D.V., 2002. Assessing copper thresholds for phytotoxicity and potential dietary toxicity in selected vegetable crops. J. Environ. Sci. Health B 37 (6), 625–635. https://doi.org/10.1081/pfc-120015443.

Yin, K., Hong, H., Churchman, G.J., Li, R., Li, Z., Wang, C., Han, W., 2013. Hydroxy-interlayered vermiculite genesis in Jiujiang late-pleistocene red earth sediments and significance to climate. Appl. Clay Sci. 74, 20–27. https://doi.org/10.1016/j.clay.2012.09.017.

Zhou, W., Hesterberg, D., Hansen, P.D.H., Hutchison, K.J., Sayers, D.E., 1999. Stability of copper sulfide in a contaminated soil. J. Synchrotron Radiat. 6 (3), 630–632. https://doi.org/10.1107/S0909049599001776.